J|A|C|S
ARTICLES
Published on Web 08/30/2006

The Arginine Anomaly: Arginine Radicals Are Poor Hydrogen Atom Donors in Electron Transfer Induced Dissociations

Xiaohong Chen and František Tureček*

Contribution from the Department of Chemistry, Bagley Hall, Box 351700, University of Washington, Seattle, Washington 98195-1700

Received May 25, 2006; E-mail: turecek@chem.washington.edu

Abstract: Arginine amide radicals are generated by femtosecond electron transfer to protonated arginine amide cations in the gas phase. A fraction of the arginine radicals formed (2-amino-5-dihydroguanid-1′-yl-pentanamide, **1H**) is stable on the 6.7 μs time scale and is detected after collisional reionization. The main dissociation of **1H** is loss of a guanidine molecule from the side chain followed by consecutive dissociations of the 2-aminopentanamid-5-yl radical intermediate. Intramolecular hydrogen atom transfer from the guanidinium group onto the amide group is not observed. These results are explained by ab initio and density functional theory calculations of dissociation and transition state energies. Loss of guanidine from **1H** is calculated to require a transition state energy of 68 kJ mol^{-1}, which is substantially lower than that for hydrogen atom migration from the guanidine group. The loss of guanidine competes with the reverse migration of the arginine α-hydrogen atom onto the guanidyl radical. RRKM calculations of dissociation kinetics predict the loss of guanidine to account for >95% of **1H** dissociations. The anomalous behavior of protonated arginine amide upon electron transfer provides an insight into electron capture and transfer dissociations of peptide cations containing arginine residues as charge carriers. The absence of efficient hydrogen atom transfer from charge-reduced arginine onto sterically proximate amide group blocks one of the current mechanisms for electron capture dissociation. Conversely, charge-reduced guanidine groups in arginine residues may function as radical traps and induce side-chain dissociations. In light of the current findings, backbone dissociations in arginine-containing peptides are predicted to involve excited electronic states and proceed by the amide superbase mechanism that involves electron capture in an amide π^* orbital, which is stabilized by through-space coulomb interaction with the remote charge carriers.

Introduction

Interactions of electrons with gas-phase cations[1] result in excitation and dissociation that forms the basis of tandem mass spectrometric techniques called electron-capture dissociation (ECD)[2] and electron-transfer dissociation (ETD).[3] In addition to the analytical utility of ECD and ETD for protein structure elucidation,[4] the electron attachment phenomena raise tantalizing fundamental questions regarding the electronic states and reactivity of the gas-phase intermediates with open electron shells. ECD and ETD are typically performed on multiply charged cations produced by electrospray ionization of biomolecules, such as peptides, proteins, saccharides, and their conjugates. These are even-electron, closed-electronic shell cations that arise by multiple protonation or cation attachment to the biomolecules in electrospray.[5] Electron attachment to such species reduces the charge state of the cation and forms an open-shell cation radical that can undergo various dissociations. In particular, ECD/ETD of peptide and protein cations typically, but not exclusively, produces fragments arising by cleavage of bonds between the amide nitrogen and the adjacent carbon atom at the C-terminus side, the N$-$C$_\alpha$ bonds. Because this dissociation often affects several N$-$C$_\alpha$ bonds in the peptide ion, it represents a useful tool for determining the amino acid sequence, which is often complementary to sequencing methods based on even-electron ion dissociations.[4]

The mechanism of the N$-$C$_\alpha$ bond cleavage in peptide cation-radicals has been the subject of several experimental and computational studies, as summarized recently.[6] Currently, there are two basic competing mechanisms explaining N$-$C$_\alpha$ bond cleavage. The first of these was originally formulated by a Cornell group[2,4a] and is hereinafter referred to as the Cornell mechanism. This presumes electron capture in a charged group of the peptide ion, followed by hydrogen transfer to a proximate amide carbonyl forming an aminoketyl intermediate (Scheme

(1) (a) Freiser, B. S.; Beauchamp, J. L. *Chem. Phys. Lett.* **1976**, *42*, 380−382. (b) Freiser, B. S. *Int. J. Mass Spectrom. Ion Phys.* **1978**, *26*, 39−47. (c) Cody, R. B.; Freiser, B. S. *Anal. Chem.* **1979**, *51*, 547−551.
(2) Zubarev, R. A.; Kelleher, N. L.; McLafferty, F. W. *J. Am. Chem. Soc.* **1998**, *120*, 3265−3266.
(3) Coon, J. J.; Ueberheide, B.; Syka, J. E. P.; Dryhurst, D. D.; Ausio, J.; Shabanowitz, J.; Hunt, D. F. *Proc. Natl. Acad. Sci. U.S.A.* **2005**, *102*, 9463−9468.
(4) (a) Zubarev, R. A.; Horn, D. M.; Fridriksson, E. K.; Kelleher, N. L.; Kruger, N. A.; Lewis, M. A.; Carpenter, B. K.; McLafferty, F. W. *Anal. Chem.* **2000**, *72*, 563−573. (b) Zubarev, R. A. *Mass Spectrom. Rev.* **2003**, *22*, 57−77. (c) Meng, F.; Forbes, A. J.; Miller, L. M.; Kelleher, N. L. *Mass Spectrom Rev.* **2005**, *24*, 126−134. (d) Cooper, H. J.; Hakansson, K.; Marshall, A. G. *Mass Spectrom. Rev.* **2005**, *24*, 201−222.
(5) Yamashita, M.; Fenn, J. B. *J. Phys. Chem.* **1984**, *88*, 4451−4459.
(6) Syrstad, E. A.; Tureček, F. *J. Am. Soc. Mass Spectrom.* **2005**, *16*, 208−224.

10.1021/ja063676o CCC: $33.50

Scheme 1

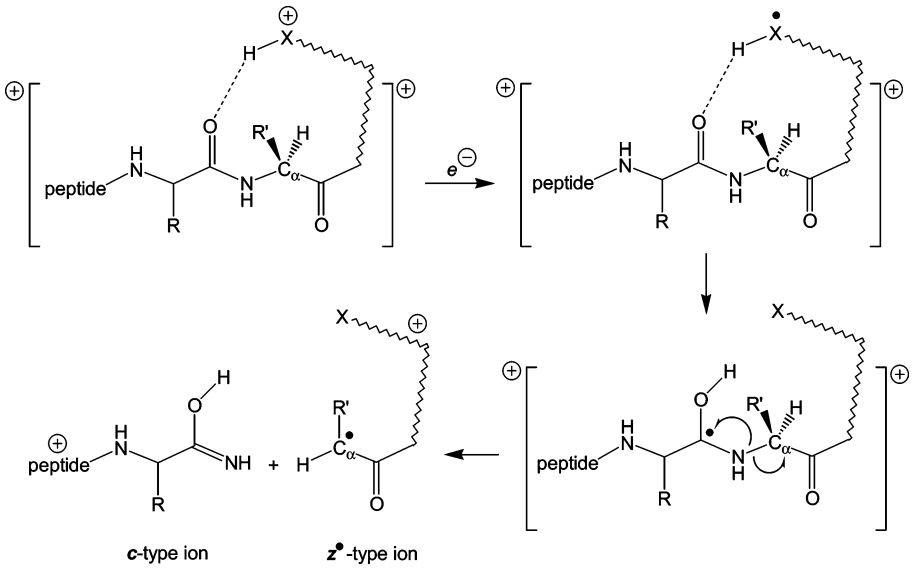

1). The latter undergoes a β-fission,[7] breaking the N−C_α bond and forming incipient fragments denoted as a ***c*** ion (even-electron N-terminal fragment) and a $z^\bullet$ ion (an open-shell C-terminal fragment). Although the Cornell mechanism had been suggested ad hoc,[2] it has received support from computational studies of N−C_α bond dissociations in model amide and peptide cation-radical systems containing ammonium groups.[8−11] These revealed that intramolecular hydrogen transfer from a charge-reduced ammonium group, such as that in the side chain of a protonated lysine residue, required a very low energy barrier in the transition state and followed the proton-coupled electron-transfer mechanism.[8] Furthermore, the aminoketyl intermediates were found to be only weakly bound and required very low transition state energies to dissociate exothermically to form ion−molecule complexes of the incipient ***c*** and $z^\bullet$ fragments.[9,12] The ion−molecule complexes can further undergo hydrogen transfers between the incipient ***c*** and $z^\bullet$ fragments that result in hydrogen exchange between the C_α positions[13] and cascade-like dissociations that have been observed experimentally.[14] Although the Cornell mechanism can account for peptide dissociations involving internally solvated lysine residues, it fails to explain backbone dissociations at amide groups that are remote from the charge sites.

The other mechanism has been proposed independently by the groups of Simons[15] and Tureček[6] and is hereinafter referred

Scheme 2

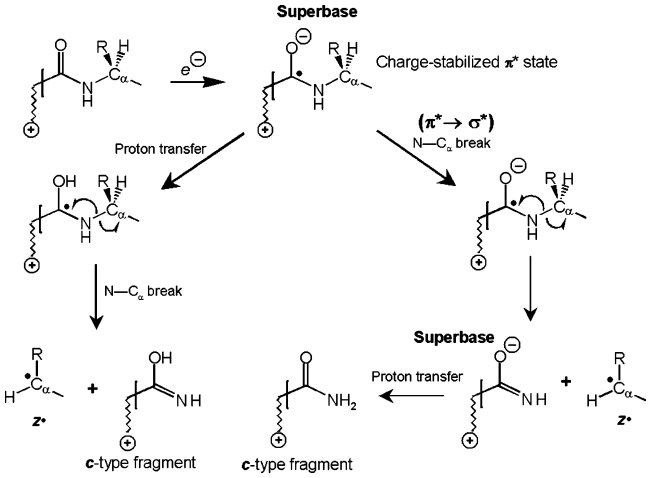

to as the Utah−Washington mechanism, or UW for short. The UW mechanism considers electron capture in a π^* orbital delocalized over an amide group to give an electronic excited state of the charge-reduced cation-radical. Such states are unbound in neutral amides that have negative electron affinities.[6] However, in a peptide cation-radical, an electron in the amide π^* excited state is stabilized by Coulomb effects of charged groups that are effective over distances greater than 15 Å. Charge-stabilized amide π^* excited states in model cation-radicals have been calculated to be bound but also extremely basic, with proton affinities (PA) exceeding 1200 kJ mol^{-1}.[6] These amide superbases can exothermically abstract a proton from a proximate proton donor group to form fragile aminoketyl radicals (Scheme 2), thus triggering backbone dissociation.[6] Alternatively, a charge-stabilized amide π^* excited state can undergo an N−C_α bond cleavage, forming an enole-imidate anion, which is also a superbase (PA > 1400 kJ mol^{-1}) and can be stabilized by abstracting a proton from a suitable intramolecular donor to form a ***c*** fragment (Scheme 2). Note that these two variants of the UW mechanism would form different tautomers of the ***c*** fragments and, thus, are potentially distinguishable by experiment. A salient feature of the UW mechanism is that it is *independent of the chemical nature of*

(7) (a) Gatlin, C. L.; Tureček, F.; Vaisar, T. *J. Am. Chem. Soc.* **1995**, *117*, 3637−3638. (b) Gatlin, C. L.; Rao, R. D.; Tureček, F.; Vaisar, T. *Anal. Chem.* **1996**, *68*, 263−270. (c) Vaisar, T.; Gatlin, C. L.; Rao, R. D.; Seymour, J. L.; Tureček, F. *J. Mass Spectrom.* **2001**, *36*, 306−316.
(8) Tureček, F.; Syrstad, E. A. *J. Am. Chem. Soc.* **2003**, *125*, 3353−3369.
(9) Tureček, F. *J. Am. Chem. Soc.* **2003**, *125*, 5954−5963.
(10) Bakken, V.; Helgaker, T.; Uggerud, E. *Eur. J. Mass Spectrom.* **2004**, *10*, 625−638.
(11) Konishi, H.; Yokotake, Y.; Ishibashi, T. *J. Mass Spectrom. Soc. Jpn.* **2002**, *50*, 229−232.
(12) Tureček, F.; Syrstad, E. A.; Seymour, J. L.; Chen, X.; Yao, C. *J. Mass Spectrom.* **2003**, *38*, 1093−1104.
(13) O'Connor, P. B.; Lin, C.; Cournoyer, J. J.; Pittman, J. L.; Belyayev, M.; Budnik, B. A. *J. Am. Soc. Mass Spectrom.* **2006**, *17*, 576−585.
(14) Leymarie, N.; Costello, C. E.; O'Connor, P. B. *J. Am. Chem. Soc.* **2003**, *125*, 8949−8958.
(15) (a) Sobczyk, M.; Anusiewicz, I.; Berdys-Kochanska, J.; Sawicka, A.; Skurski, P.; Simons, J. *J. Phys. Chem. A* **2005**, *109*, 250−258. (b) Anusiewicz, I.; Berdys-Kochanska, J.; Simons, J. *J. Phys. Chem. A* **2005**, *109*, 5801−5813. (c) Anusiewicz, I.; Berdys-Kochanska, J.a; Skurski, P.; Simons, J. *J. Phys. Chem. A* **2006**, *110*, 1261−1266. (d) Sobczyk, M.; Simons, J. *J. Phys. Chem. B* **2006**, *110*, 7519−7527.

Scheme 3

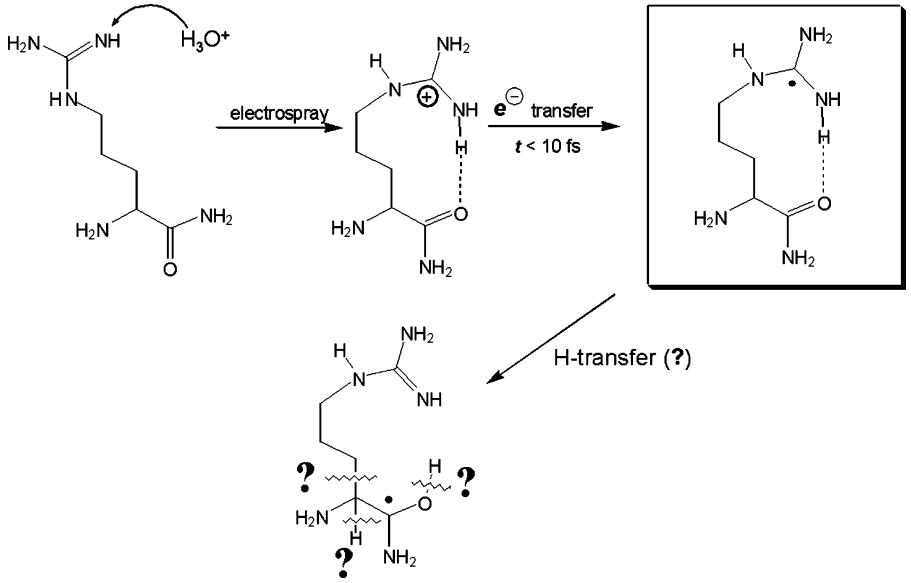

the charge-carrying groups, which, depending on the peptide composition, can be the N-terminal or lysine ammonium, arginine guanidinium, histidine imidazolium, or a backbone-protonated amide group. In contrast, in the Cornell mechanism, the charge-carrying group is involved in the proton-coupled electron transfer, and so the transition state energy and, hence, the dissociation kinetics may depend on the electronic properties of the protonated and charge-reduced site. This is particularly pertinent to hydrogen atom transfers from protonated arginine and histidine residues for which no mechanistic studies have been reported by experiment or theory.

In an effort to shed some light on the existing dichotomy in the ECD mechanisms, we now report an experimental and computational study of arginine radicals. We chose arginine amide as a simple model system which is expected to be protonated at the basic guanidine group in both solution and the gas phase (Scheme 3). The charged guanidinium group is further expected to gain stabilization by internal solvation through hydrogen bonding to the amide group. Thus, the guanidinium and amide moieties are in a close proximity in the parent ion prior to electron transfer. The latter is accomplished in a single collision occurring on a femtosecond time scale,[16] so that the incipient radical has the geometry of the precursor ion including the hydrogen bonding interactions. Further development of the system on the radical potential energy surface and branching into the dissociation channels is monitored on the microsecond time scale using neutralization-reionization mass spectrometry that provides practically complete product analysis.[17,18] By identifying the products of radical dissociations one can establish the probable mechanisms of radical dissociations and thus elucidate whether the radical underwent intramolecular hydrogen transfer from the guanidinium group to the amide group. The principal advantage of the present system over arginine-containing peptide models[19,20] is that it entirely avoids $N-C_\alpha$ bond cleavage that might be triggered by either the Cornell or UW mechanisms, and thus it solely probes the propensity of the arginine guanidinium group for hydrogen transfer to the amide carbonyl, which is critical for the Cornell mechanism only. We show that the guanidinium group is an inefficient hydrogen atom donor and we provide theoretical justification of this experimental finding.

Experimental Section

Materials. Arginine amide dihydrochloride was purchased from Bachem California, Inc. (Torrance, CA, https://www.bachem.com) and used as received. $H_2{}^{18}O$ (97% ^{18}O) was purchased from Cambridge Isotope Laboratories (Andover, MA, http://www.isotope.com). Methanol (Fisher Scientific, HPLC grade) was distilled in Pyrex to remove sodium salts.

Arginine amide-^{18}O was prepared as follows. Arginine amide dihydrochloride (46 mg, 185 μmol) was added to 1.3 g $H_2{}^{18}O$ that was made acidic by adding 45 μL $SOCl_2$, and the solution was heated at 90 °C under stirring in a closed vessel overnight. An aliquot was analyzed by ESI-MS and showed clean formation of arginine-$^{18}O_2$ as characterized by an $(M + H)^+$ ion at *m*/*z* 179. Then, the reaction mixture was brought to dryness in vacuo, 20 mL of anhydrous methanol was added with a few drops of H_2SO_4, and the mixture was refluxed overnight. The product was analyzed by ESI-MS to show a single peak of $(M + H)^+$ ion at *m*/*z* 190 corresponding to the ^{18}O isotopomer of arginine methyl ester. The methanol solution of the latter was saturated with gaseous anhydrous NH_3, the solution was placed in a stainless steel pressure vessel and heated overnight at 80 °C. After cooling and depressurizing, the solvent was evaporated, the product was taken in distilled water and purified by HPLC using gradient elution with water/acetonitrile.

Methods. Electrospray mass spectra were taken on a Bruker Esquire quadrupole ion trap and ABI−Sciex API-4000 triple quadrupole mass

(16) Tureček, F. *Top. Curr. Chem.* **2003**, *225*, 77−129.
(17) (a) Curtis, P. M.; Williams, B. W.; Porter, R. F. *Chem. Phys. Lett.* **1979**, *65*, 296−299. (b) Burgers, P. C.; Holmes, J. L.; Mommers, A. A.; Terlouw, J. K. *Chem. Phys. Lett.* **1983**, *102*, 1−3. (c) Danis, P. O.; Wesdemiotis, C.; McLafferty, F. W. *J. Am. Chem. Soc.* **1983**, *105*, 7454−7456.
(18) For recent reviews, see: (a) Zagorevskii, D. V. In *Comprehensive Coordination Chemistry II*; McCleverty, J. A., Meyer, T. J., Eds.; Elsevier: Oxford, 2004; pp 381−386. (b) Tureček, F. In *Encyclopedia of Mass Spectrometry*; Armentrout, P. B., Ed.; Elsevier: Amsterdam, 2003; Vol. 1, Chapter 7, pp 528−541. (c) Zagorevskii, D. V. *Coord. Chem. Rev.* **2002**, *225*, 5−34. (d) Gerbaux, P.; Wentrup, C.; Flammang, R. *Mass Spectrom. Rev.* **2000**, *19*, 367−389. (e) Zagorevskii, D. V.; Holmes, J. L. *Mass Spectrom. Rev.* **1999**, *18*, 87−118. (f) Schalley, C.; Hornung, G.; Schröder, D. Schwarz, H. *Chem. Soc. Rev.* **1998**, *27*, 91−104.
(19) Cooper, H. J. *J. Am. Soc. Mass Spectrom.* **2005**, *16*, 1932−1940.
(20) Fung, Y. M. E.; Chan, T.-W. D. *J. Am. Soc. Mass Spectrom.* **2005**, *16*, 1523−1535.

spectrometers equipped with electrospray ion sources. Samples were introduced as 5 μmol methanol solutions. Collision-induced dissociation (CID) mass spectra were obtained with argon as collision gas at laboratory collision energies ranging from 20 to 50 eV. Neutralization-reionization ($^{+}NR^{+}$) mass spectra were measured on a tandem quadrupole acceleration−deceleration mass spectrometer described previously.[21] Ions were produced by electrospraying 100 μM arginine amide solutions in 90/9/1 methanol/water/acetic acid in a special ionizer attached to the tandem instrument.[22] The ions were transmitted by a glass-lined stainless steel capillary (0.8 mm i.d., Scientific Instrument Services,) to the first vacuum chamber (0.25−0.4 Torr) housing an electrodynamic ion funnel lens.[22,23] After passing a 2-mm conductance limit, the ions were transmitted by an r.f.-only octopole ion guide to the high-vacuum housing where they were injected into a quadrupole mass analyzer. The ions emerging from the analyzer were accelerated to 7170 keV and focused on the first collision chamber where a fraction was discharged by collisions with dimethyl disulfide that was admitted at pressures allowing 70% transmittance of the ion beam. According to Poisson statistics, this corresponds to 83% single collisions. The remaining ions were reflected by a cylindrical lens floated at +250 eV, and the neutral beam was allowed to drift to the second collision cell located 60 cm down beam. Neutral species in the fast beam were nonselectively ionized by collisions with oxygen that was admitted at pressures allowing 70% transmittance of the beam. The resulting cations were decelerated to 75−80 eV, energy filtered and mass analyzed by a quadrupole mass filter that was floated at 70−75 V and operated at unit mass resolution. The reported $^{+}NR^{+}$ mass spectra were averaged over 100−150 consecutive scans taken with 200 data points per mass unit.

Calculations. Standard ab initio and density functional theory calculations were performed using the Gaussian 03 suite of programs.[24] Geometries were optimized with B3LYP[25] and the 6-31+G(d,p) basis set. Tables of complete optimized structures are available as Supporting Information. Local energy minima and transition states were characterized by harmonic frequency analysis to have the appropriate number of imaginary frequencies (zero for local minima and one for transition states). Improved energies were obtained by single-point calculations on the B3LYP-optimized geometries. The single-point calculations used B3LYP and Møller−Plesset perturbational theory truncated at second order with valence electrons only excitations (MP2(frozen core)) and basis sets of triple-ζ quality, 6-311++G(2d,p), 6-311++G(3df,2p), and aug-cc-pVTZ.[26] For the molecular systems of the arginine amide radical size, these basis sets comprised 648, 888, and 1308 primitive Gaussians, respectively. Spin unrestricted formalism was used for calculations of open-shell systems. Contamination by higher spin states was modest, as judged from the expectation values of the spin operator $\langle S^2 \rangle$ that were $\leq$0.76 for UB3LYP and $\leq$0.78 for UMP2 calculations. The UMP2 energies were corrected by spin annihilation[27] that reduced the $\langle S^2 \rangle$ to close to the theoretical value for a pure doublet state (0.75). Spin annihilation lowered the total MP2 energies by 2 millihartree (5.3 kJ mol^{-1}, root-mean-square deviation) for local energy minima and by 14 millihartree (37 kJ mol^{-1}) for transition states. The single point B3LYP and spin-projected MP2 energies were averaged according to the B3−PMP2 procedure[28] that results in cancellation of small errors inherent to both approximations and provides dissociation and transition state energies of improved accuracy as has been previously shown for a number of closed-shell and open-shell systems.[29] Excited-state energies were calculated with time-dependent density functional theory[30] using the B3LYP functional and the 6-311++G(2d,p) basis set. Atomic spin and charge densities were calculated using the natural population analysis (NPA) method.[31]

Unimolecular rate constants were calculated by the Rice−Ramsperger−Kassel−Marcus (RRKM)[32] theory using Hase's program[33] that was recompiled for Windows NT.[34] The RRKM rate constants were obtained by direct count of quantum states at internal energies that were increased in 2 kJ mol^{-1} steps from the transition state up to 400 kJ mol^{-1} above the reactant. Rotations were treated adiabatically, and the calculated *k(E,J,K)* microscopic rate constants were Boltzmann-averaged over the thermal distribution of rotational states at 298 K, corresponding to the ion source temperature, to provide canonical rate constants *k*(*E*).

Results

Arginine Amide Structure and Energetics. Arginine amide is both the starting molecule of the reported experiments and one of the expected dissociation products of arginine amide radicals, and so its gas-phase structure was of interest. DFT calculations with gradient optimizations provided several local energy minima (**1**−**5**, Figure 1, Table 1) that differed in the side chain conformations and also included guanidine tautomers. The lowest free-energy structure (**1**) has an *anti*-conformation of the side chain and an *exo*-imine group in the guanidine moiety (Figure 1). Interestingly, intramolecular hydrogen bonding of the side chain in arginine amide (**3**) is disfavored both thermochemically, $\Delta H^{\circ}_{g,298}$(**1** → **3**) = 14 kJ mol^{-1}, and thermodynamically, $\Delta G^{\circ}_{g,298}$ (**1** → **3**) = 22 kJ mol^{-1} (Table 1). Thus, arginine amide differs from the free amino acid that prefers folded structures in which the carboxylic hydroxyl is hydrogen bonded to the *endo*- and *exo*-imine nitrogens of the guanidine group.[35]

Arginine Amide Cations and Radicals. Protonation of **1** occurs in the guanidine group with proton affinities (PA) in the range of 1014−1049 kJ mol^{-1} for the various ion conformers (Table 2). In contrast, the α-amino group is less basic (*PA* = 958−960 kJ mol^{-1}) and is not expected to be protonated in the gas-phase cations. The most stable ion conformer is stabilized by intramolecular H-bonding to the amide carbonyl (**1H**$^{+}$, Figure 1). This stabilization amounts to $\Delta H^{\circ}_{g,298}$ = −25.9 kJ mol^{-1} and $\Delta G^{\circ}_{g,298}$ = −12.5 kJ mol^{-1} when referred to the most stable unfolded conformer **2H**$^{+}$ (Figure 1). The calculated proton affinities and ion relative free energies indicate that protonated arginine amide that is produced by electrospray has the proton

(21) (a) Tureček, F.; Gu, M.; Shaffer, S. A. *J. Am. Soc. Mass Spectrom.* **1992**, *3*, 493−501. (b) Tureček, F. *Org. Mass Spectrom.* **1992**, *27*, 1087−1097.
(22) Seymour, J. L.; Syrstad, E. A.; Langley, C. C.; Tureček, F. *Int. J. Mass Spectrom.* **2003**, *228*, 687−702.
(23) Shaffer, S. A.; Tang, K.; Anderson, G. A.; Prior, D. C.; Udseth, H. R.; Smith, R. D. *Rapid Commun.* Mass Spectrom. **1997**, *11*, 1813−1817.
(24) Frisch, M. J.; et al. *Gaussian 03*, revision B.05; Gaussian, Inc.; Pittsburgh, PA, 2003.
(25) (a) Becke, A. D. *J. Chem. Phys.* **1993**, *98*, 1372−1377. (b) Becke, A. D. *J. Chem. Phys.* **1993**, *98*, 5648−5652. (c) Stephens, P. J.; Devlin, F. J.; Chabalowski, C. F.; Frisch, M. J. *J. Phys. Chem.* **1994**, *98*, 11623−11627.
(26) Dunning, T. H., Jr. *J. Chem. Phys.* **1989**, *90*, 1007−1023.
(27) (a) Schlegel, H. B. *J. Chem. Phys.* **1986**, *84*, 4530−4534. (b) Mayer, I. *Adv. Quantum Chem.* **1980**, *12*, 189−262.
(28) Tureček, F. *J. Phys. Chem. A* **1998**, *102*, 4703−4713.
(29) (a) Tureček, F.; Polásek, M.; Frank, A. J.; Sadílek. M. *J. Am. Chem. Soc.* **2000**, *122*, 2361−2370. (b) Polásek, M.; Tureček, F. *J. Am. Chem. Soc.* **2000**, *122*, 9511−9524. (c) Tureček, F.; Yao, C. *J. Phys. Chem. A* **2003**, *107*, 9221−9231. (d) Rablen, P. R. *J. Am. Chem. Soc.* **2000**, *122*, 357−368. (e) Rablen, P. R. *J. Org. Chem.* **2000**, *65*, 7930−7937. (f) Rablen, P. R.; Bentrup, K. H. *J. Am. Chem.* Soc. **2003**, *125*, 2142−2147. (g) Hirama, M.; Tokosumi, T.; Ishida, T.; Aihara, J. *Chem. Phys.* **2004**, *305*, 307−316.
(30) Stratmann, R. E.; Scuseria, G. E.; Frisch, M. J. *J. Chem. Phys.* **1998**, *109*, 8218−8224.
(31) Reed, A. E.; Weinstock, R. B.; Weinhold, F. *J. Chem. Phys.* **1985**, *83*, 735−745.
(32) Gilbert, R. G.; Smith, S. C. *Theory of Unimolecular and Recombination Reactions*; Blackwell Scientific Publications: Oxford, 1990; pp 52−132.
(33) Zhu, L.; Hase, W. L. *Quantum Chemistry Program Exchange*; Indiana University: Bloomington, 1994; Program No. QCPE 644.
(34) Frank, A. J.; Sadílek, M.; Ferrier, J. G.; Tureček, F. *J. Am. Chem. Soc.* **1997**, *119*, 12343−12353.
(35) Gdanitz, R. J.; Cardoen, W.; Windus, T. L.; Simons, J. *J. Phys. Chem. A* **2004**, *108*, 515−518.

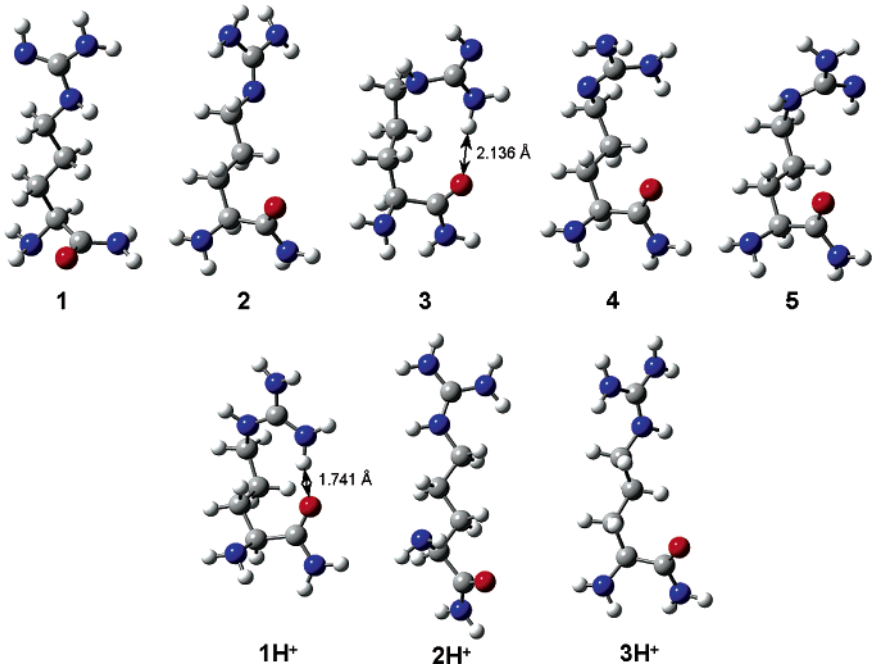

Figure 1. B3LYP/6-31+G(d,p) optimized strructures of **1**−**5**, **1H**$^+$ and **2H**$^+$.

Table 1. Arginine Energetics

	relative energy[a]			
	B3LYP	B3-MP2		
arginine amide isomer	6-31+G(d,p)	6-311++G(2d,p)	6-311++G(3df,2p)	aug-cc-pVTZ
1	0	0	0	0
2	9 (7)[b]	7 (5)	8 (6)	8 (6)
3	18 (26)	15 (23)	15 (23)	14 (22)
4	19 (20)	16 (16)	16 (16)	16 (17)
5	18 (17)	15 (14)	15 (14)	15 (14)

[a] Including B3LYP/6-31+G(d,p) zero-point vibrational energies and 298 K enthalpies and referring to 298 K. [b] Values in parentheses are the 298 K relative free energies, $\Delta G^\circ_{g,298}$.

Table 2. Arginine Amide Protonation Energetics

	relative energy[a]			
	B3LYP	B3-MP2		
reaction	6-31+G(d,p)	6-311++G(2d,p)	6-311++G(3df,2p)	aug-cc-pVTZ
1H$^+$ → **1** + H$^+$	1053 (1012)[b]	1043 (1001)[b]	1046 (1005)[b]	1049 (1006)[b]
2H$^+$ → **1** + H$^+$	1034	1020	1024	1022
3H$^+$ → **1** + H$^+$	1023	1012	1017	1014

[a] Proton affinities including B3LYP/6-31+G(d,p) zero-point vibrational energies and 298 K enthalpies and referring to 298 K. [b] Gas-phase basicities at 298 K.

attached to the guanidine group and assumes the folded conformation **1H**$^+$.

Collisional electron transfer to **1H**$^+$ gives rise to intermediate radical **1H** that undergoes substantial dissociation on the time scale of the experiment (6.7 μs). Note that electron transfer from the dimethyl disulfide donor (IE_{vert} = 8.96 eV)[36] to **1H**$^+$ (RE_{vert} = 2.67 eV) is substantially endoergic, ΔE = 8.96−2.67 = 6.29 eV (607 kJ mol^{-1}), and is possible only in fast collisions where the energy deficit is compensated by conversion of a small fraction of the available center-of-mass kinetic energy of the system (E_{COM} = 2525 eV). The $^+$NR$^+$ mass spectrum (Figure 2a) showed a weak peak of the survivor ion for **1H**$^+$ at *m*/*z* 174 that indicated that there was a fraction of nondissociating radicals **1H** with lifetimes of ≥6.7 μs that were reionized and detected as cations. The identity of **1H**$^+$ was corroborated by a mass shift to *m*/*z* 176 for the ^{18}O-labeled ion (Figure 2a, inset), and the presence of an abundant fragment at *m*/*z* 70. The latter is the dominant product of collision-induced dissociation of **1H**$^+$ (Figure 2b) and its presence in the $^+$NR$^+$ mass spectrum strongly indicates that **1H**$^+$ is formed by reionization of **1H**. Although ion dissociations were not the primary focus of this work, the ^{18}O labeling data (Figure 2c) clearly provided clues to disentangling some of the dissociation pathways of **1H**$^+$, as summarized for reference in Scheme 4. In particular, heterolysis of the side-chain C_δ−N bond in **1H**$^+$ gives rise to the comple-

(36) NIST Standard Reference Database Number 69 − March, 2003 Release; http://webbook.nist.gov/chemistry.

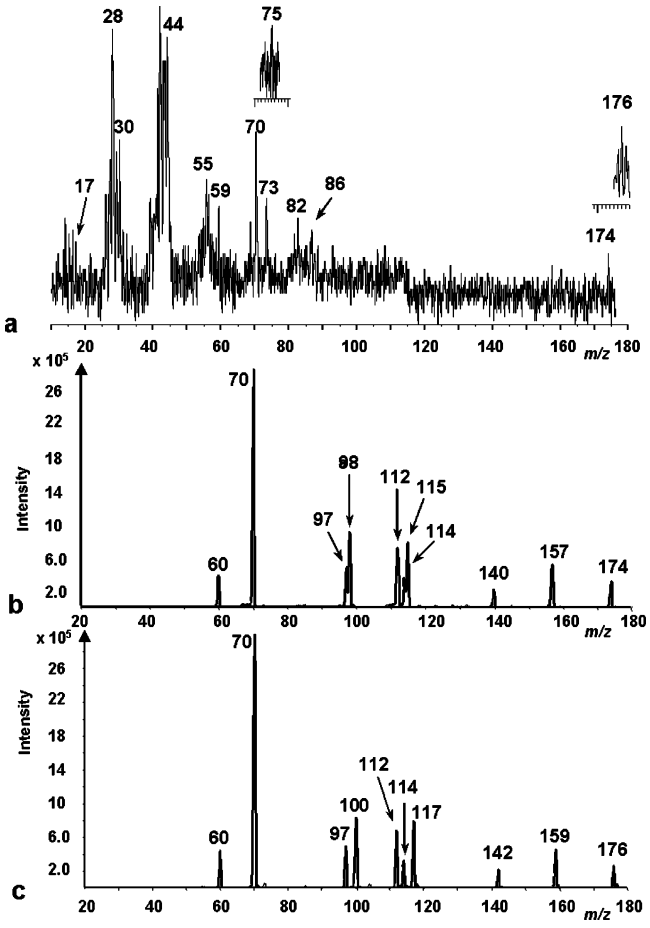

Figure 2. (a) Neutralization (CH_3SSCH_3, 70% T)/reionization (O_2, 70% T) mass spectrum of $\mathbf{1H}^+$. (Insets) Relevant regions in the $^+NR^+$ mass spectrum of an ^{18}O-labeled ion. Collision-induced dissociation mass spectra of (b) $\mathbf{1H}^+$ and (c) ^{18}O-$\mathbf{1H}^+$.

Scheme 4

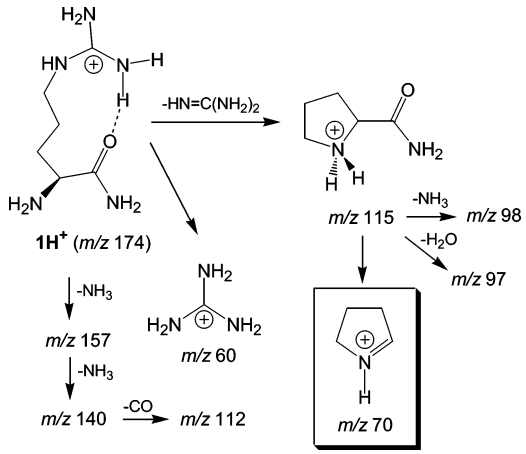

mentary *m*/*z* 115 and 60 fragments. The former dissociates further by elimination of CO and NH_3 to form the *m*/*z* 70 ion.

The major part of the $^+NR^+$ mass spectrum comprised reionized products of radical dissociations at *m*/*z* 86, 82, 73, 59, 44, 43, 42, 30, and 28. The dissociations showed a side-chain cleavage resulting in the formation of guanidine that appeared at *m*/*z* 59 after collisional reionization (Scheme 5). Ionized guanidine further dissociated to form the *m*/*z* 43, 42, and 28 fragments that were also observed in the $^+NR^+$ mass spectrum. This dissociation sequence was established from the

Scheme 5

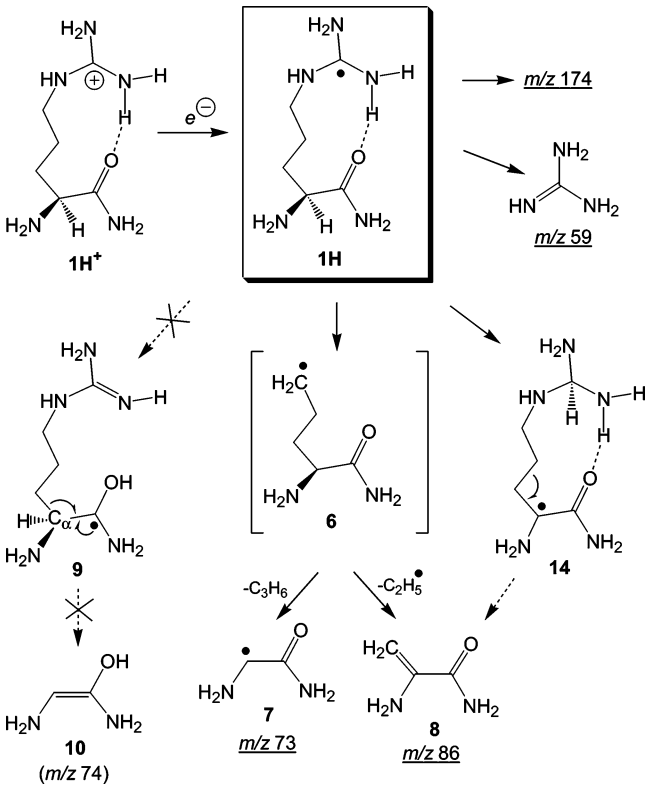

collision-induced dissociation of an authentic guanidine cation-radical (Figure S1, Supporting Information). Interestingly, a radical fragment (**6**, Scheme 5) complementary to the guanidine molecule was not observed at *m*/*z* 115. Rather, the latter underwent consecutive dissociation forming the stable glycine-2-yl amide radical (**7**) that appeared at *m*/*z* 73 after reionization (Scheme 5). Fragment **7** ($C_2H_5N_2O$) was distinguished from the nominally isobaric methylguanidine ($C_2H_7N_3$) by the mass shift to *m*/*z* 75 in the $^+NR^+$ mass spectrum of ^{18}O-labeled arginine amide (Figure 1a, inset). The identity of radical **7** was further corroborated by the $^+NR^+$ mass spectra of related glycin-2-yl, glycin-2-yl methyl ester, and glycin-2-yl-*N*-methylamide radicals that have been shown to be kinetically and thermodynamically stable when formed by fast electron transfer in the gas phase.[37] Loss of an ethyl radical from **6** accounted for the formation of another stable fragment, 2-aminopropenamide (**8**, Scheme 5) at *m*/*z* 86, although the latter can also be formed by an alternative pathway via intermediate **14** (Scheme 5), as discussed below.

A salient feature of the radical dissociations is the absence of fragments that would have resulted from an intramolecular transfer of a guanidinium hydrogen atom to the amide carbonyl. Scheme 5 shows that such a hydrogen transfer would be expected to produce an aminoketyl radical intermediate (**9**) that would undergo a β-fission of some of the adjacent $C_\alpha-C_\beta$, $C_\alpha-H$, $C_\alpha-N$, O−H, or N−H bonds yielding stable molecules as products. For example, β-fission of the $C_\alpha-C_\beta$ bond would be expected to form the very stable enol of glycine amide (**10**) that would have been readily detectable in the $^+NR^+$ mass

(37) (a) Carpenter, F. H.; Tureček, F. *J. Chem. Soc., Perkin Trans. 2* **1999**, 2315−2323. (b) Tureček, F.; Carpenter, F. H.; Polce, M. J.; Wesdemiotis, C. *J. Am. Chem. Soc.* **1999**, *121*, 7955−7956. (c) O'Hair, R. A. J.; Blanksby, S.; Styles, M.; Bowie, J. H. *Int. J. Mass Spectrom.* **1999**, *182/183*, 203−211. (d) Polce, M. J.; Wesdemiotis, C. *J. Am. Soc. Mass Spectrom.* **1999**, *10*, 1241−1247.

Scheme 6

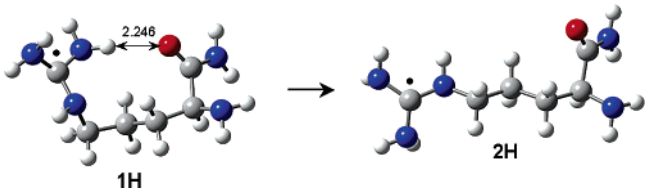

spectrum at *m*/*z* 74.[38,39] The absence of the corresponding fragment in the $^{+}NR^{+}$ mass spectrum at the current signal-to-noise level strongly indicated that the requisite aminoketyl intermediate **9** was not formed as a major species. Thus, we conclude that intramolecular hydrogen transfer from the guanidinium moiety is inefficient and does not compete with simple bond dissociations in arginine radicals.

Arginine Amide Radical Geometries and Electronic Structure. The radical dissociations observed upon fast electron transfer can be interpreted on the basis of the calculated geometries, electronic structures, and dissociation and transition state energies for the relevant species. Electron capture in ion $\mathbf{1H}^{+}$ results in significant changes in the molecular geometry in the relaxed radical **1H**. In particular, the intramolecular H-bond between the guanidinium moiety and the amide carbonyl is weakened, as indicated by the increased O···H distance from 1.741 Å in $\mathbf{1H}^{+}$ (Figure 1) to 2.246 Å in **1H** (Scheme 6). As a result of this weakening, unfolding of the side chain to form radical conformer **2H** was calculated to be thermodynamically favorable, $\Delta G°_{g,298} = -3.9$ kJ mol^{-1}. This suggests that, following electron capture and geometry relaxation, the guanidinium radical moiety will be remote from the amide group in a >50% fraction of charged-reduced species corresponding to **2H**. The other substantial geometry changes from $\mathbf{1H}^{+}$ to **1H** are the pyramidization of the guanidine central carbon atom and lengthening of the N−C bonds. Thus, whereas the guanidinium N−C═$(N)_2$ framework is planar in $\mathbf{1H}^{+}$ and in incipient **1H** when produced by vertical electron transfer, the relaxed structure of **1H** shows 34° pyramidization, when expressed as the angle between the *endo* N−C bond and the N−C−N plane. The guanidinium N−C bond lengths increase from 1.332−1.349 Å in $\mathbf{1H}^{+}$ to 1.405−1.421 Å in relaxed **1H**. The differences in the relaxed geometries of $\mathbf{1H}^{+}$ and **1H** result in Franck−Condon effects, so that the vertically formed **1H** acquires 68 kJ mol^{-1} vibrational energy upon electron transfer.

The electronic structure of **1H** was studied by calculating the molecular orbitals for the ground and several lowest electronic excited states in both the relaxed and vertically reduced radicals (Figure 3a,b). The highest singly occupied molecular orbital (SOMO) in the relaxed radical **1H** (Figure 3a) is a guanidinium π orbital which shows negligible delocalization over the rest of the molecule. This is also illustrated by atomic spin densities calculated by natural population analysis that show 98% of unpaired electron density to be in the guanidinium group with a major component (68%) at the carbon atom and the remaining 30% delocalized over the hydrogen and

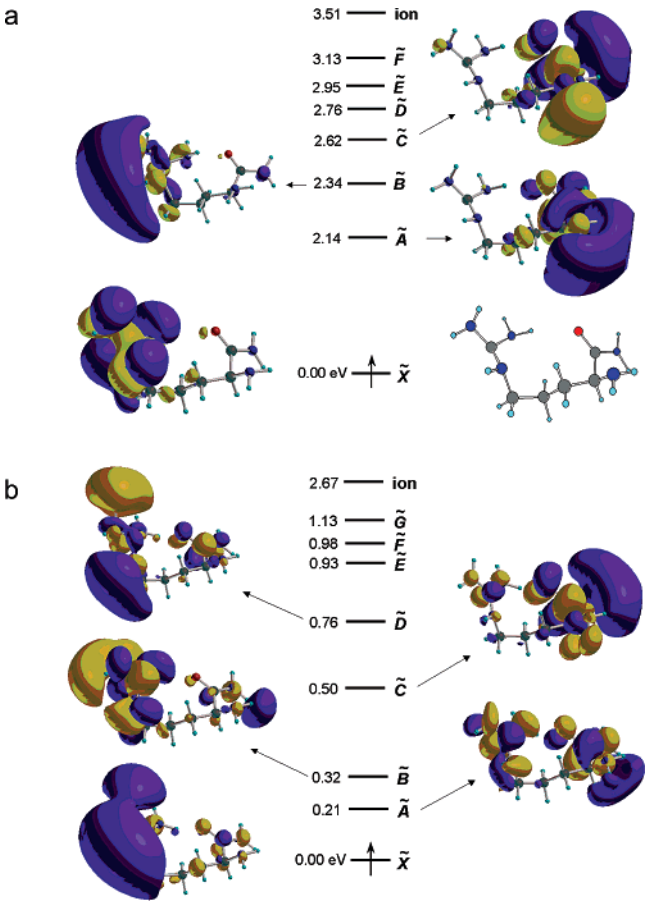

Figure 3. Molecular orbitals and electronic states in (a) relaxed radical **1H** and (b) **1H** formed by vertical electron transfer to $\mathbf{1H}^{+}$. The excitation energies in eV are from TD-B3LYP/6-311++G(2d,p) single point calculations.

nitrogen atoms. The first (*A*) and third (*C*) excited states in **1H** arise by mixing the amide π^* orbital with the amino group 3s and 3p Rydberg-like orbitals, respectively. The *B* state consists mainly of a combination of 2s Rydberg-like orbitals on the guanidinium hydrogen atoms. The vertical excitation energy, $\Delta E_{exc}(X \rightarrow A) = 2.14$ eV (206 kJ mol^{-1}), is sufficiently large to separate the local energy minima on the ground-state potential energy surface from those of the first excited state. However, the energy gaps between the ground and excited states are substantially diminished in vertically formed **1H**.

The latter shows a dense manifold of electronic states within the 2.67 eV (258 kJ mol^{-1}) range determined by the vertical recombination energy (Figure 3b). In contrast to relaxed **1H**, the vertically formed radical shows the unpaired electron in the *X* state in a Rydberg-like orbital at the guanidinium moiety. The *B* state is represented by the guanidinium π orbital which is only 0.32 eV (31 kJ mol^{-1}) above the *X* state. The ordering of the electronic states shows that geometry relaxation in **1H** following electron transfer is accompanied by a substantial lowering of the guanidinium π orbital energy to become the ground electronic state in the fully relaxed structure.

Radical Dissociation Energetics and Kinetics. The unpaired electron in the guanidinium radical in **1H** is presumed to activate the adjacent bonds for dissociations of the β-fission type. Dissociations of the guanidine N−H bonds in **1H** were calculated by B3LYP to proceed as continuously endothermic reactions with no distinct transition states. However, mapping

(38) (a) Polce, M. J.; Wesdemiotis, C. *J. Mass Spectrom.* **2000**, *35*, 251−257. (b) Tam, F.; Syrstad, E. A.; Chen, X.; Tureček, F. *Eur. J. Mass Spectrom.* **2004**, *10*, 869−880.

(39) Amide enols such as the putative fragment **10** typically give very intense survivor ions in neutralization-reionization mass spectra (ref 16). The efficiencies in collisional reionization at keV kinetic energies scale with the number of atoms in the neutral molecule (ref 34) and should be comparable for **7** and **10** that differ by a single hydrogen atom.

Table 3. Arginine Amide Radical Energetics

	relative energy[a]			
	B3LYP	B3–PMP2		
reaction	6-31+G(d,p)	6-311++G(2d,p)	6-311++G(3df,2p)	aug-cc-pVTZ
1H → **1H**$^+$ + e$^-$	347[b]	341[b] (516)[c]	337[b] (519)[c]	339[b]
1H$^+$ + e$^-$ → **1H**		−236[d]	−258[d]	−261[d]
1H → **2H**	−2	1	1	2 (−4)[e]
1H → **4H**	9	13	13	13 (9)[e]
1H → **1** + H	80	62	62	66
1H → **4** + H	99	77	78	74
1H → **6** + HN=C(NH$_2$)$_2$	−7	14	−0.3	−0.3
1H → **9**	26	24	22	20
1H → **10** + **11**	81	97	97	95
1H → **13**	18	20	20	18
1H → **12** + HN=C(NH$_2$)$_2$	21	47	30	29
1H → **14**	−59	−56	−55	−56
1H → **15** + CH$_2$=C(NH$_2$)CONH$_2$	69	84	83	83
1H → **TS1**	–[f]	88	87	87
1H → **TS2**	63	65	66	68
1H → **TS3**	67	76	77	72
1H → **TS4**	62	74	74	78
1H → **TS5**	129	133	132	130
1H → **TS6**	121	129	129	126
1H → **TS7**	44	45	47	46
1H → **TS8**	77	84	87	85

[a] In units of kJ mol^{-1}, including zero-point vibrational energies and referring to 0 K. [b] Adiabatic ionization energies including ZPVE corrections. [c] Vertical ionization energies. [d] Vertical recombination energies. [e] $\Delta G°_{g,298}$ values. [f] The B3LYP/6-31+G(d,p) potential energy surface showed no saddle point.

Scheme 7

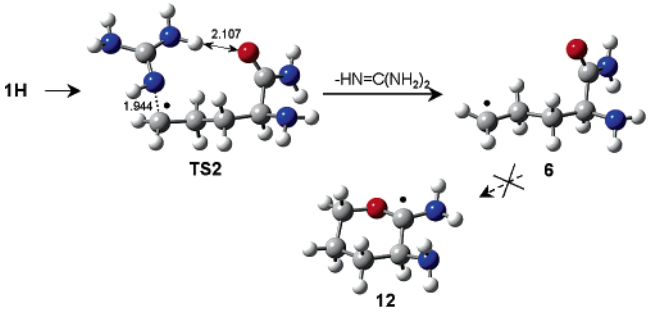

Scheme 8

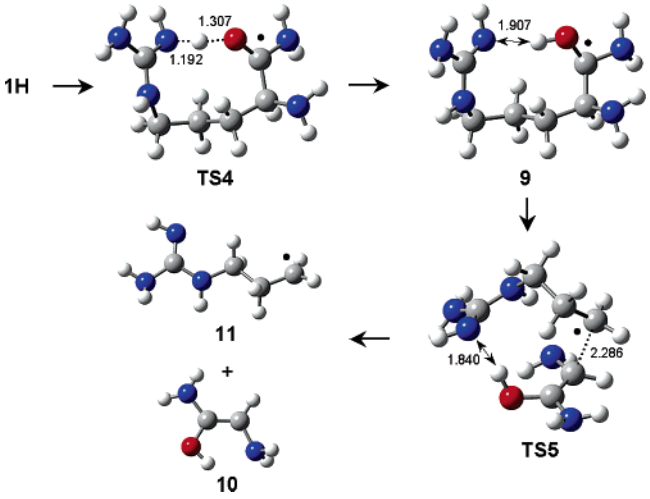

by B3−PMP2 the potential energy surface along the dissociation coordinate[40] revealed a transition state (**TS1**, Figure S2, Supporting Information) at an N−H separation of 1.635 Å that was 88 kJ mol^{-1} above **1H**. The electronic structure of **TS1** shows most of the unpaired spin density to be at the departing hydrogen atom (76%) while the remaining 23% is delocalized over the guanidine C and N atoms. The loss of the amine hydrogen atom to yield **1** requires 66 kJ mol^{-1} at the 0 K thermochemical threshold. (Table 3). β-Fission of the N−C$_\delta$ bond to form guanidine and the 2-aminopentanamid-5-yl radical (**6**) requires 68 kJ mol^{-1} in the transition state (**TS2**) that was found at an N···C separation of 1.944 Å. The **TS2** energy is somewhat lowered by the increased hydrogen bonding of the incipient guanidine moiety to the amide carbonyl, as judged by the shortened H···O distance (2.107 Å) in **TS2** relative to that in **1H** (Scheme 7). This stabilization was assessed by examining β-fission of the N−C$_\delta$ bond in the linear arginine amide radical **2H** that requires 70 kJ mol^{-1} in the transition state (**TS3**, Figure S3, Supporting Information), or 72 kJ mol^{-1} relative to **1H**. Hence, the **TS** stabilization by H bonding is only modest (4 kJ mol^{-1}). Note that the dissociation of **1H** to guanidine and **6** is nearly thermoneutral (Table 3), implying that **1H** is inherently metastable. Interestingly, cyclic radical products (**12**, Scheme 7, and its conformation isomer **13**, Figure S4, Supporting Information) are less stable than **6**, indicating that the latter does not spontaneously cyclize when formed by loss of guanidine from **1H**.

Migration of a guanidinium hydrogen atom to the amide carbonyl was found to be 20 kJ mol^{-1} endothermic to form the aminoketyl radical **9** (Scheme 8). In addition, the migration requires 78 kJ mol^{-1} in the transition state (**TS4**, Scheme 8). Population analysis of the structures along the migration coordinate shows that the spin density on the migrating hydrogen atom decreases from 4% in **1H** to 3% in **TS4** and becomes practically zero in **9**. At the same time, the atomic charge on the migrating hydrogen increases from +0.39 in **1H** to +0.44 in **TS4** to reach +0.51 in **9**. The main portion of unpaired spin density in **TS4** is found in the amide group (62%), whereas 23% remains in the guanidine moiety. The TS energy and electron distribution in the hydrogen atom migration in arginine

(40) Syrstad, E. A.; Stephens, D. D.; Tureček, F. *J. Phys. Chem. A* **2003**, *107*, 115−126. (b) Chen, X.; Syrstad, E. A.; Tureček, F. *J. Phys. Chem. A* **2004**, *108*, 4163−4173.

Scheme 9

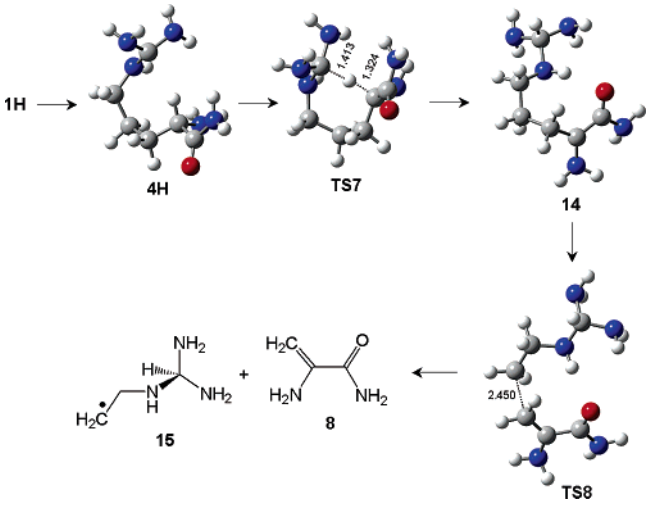

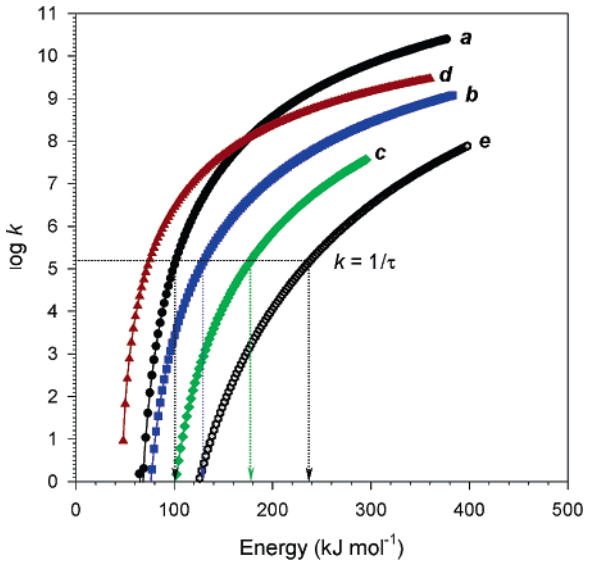

Figure 4. Plots of log *k* versus internal energy from RRKM calculations of dissociations in **1H** on the B3−PMP2/6-311++G(2d,p) potential energy surface. (a) N−C_δ bond cleavage through **TS2**. (b) N···H···O migration through **TS4**. (c) N- - -H break through **TS1**. (d) C_α···H···C(guanidine) migration through **TS7**. (e) C_β−C_γ bond cleavage in **14**.

radicals are substantially different from those reported for analogous H-atom migrations in lysine radicals. The aminoketyl radical **9** can undergo β-fission dissociations that are promoted by the unpaired electron in the amide group that carries 95% of the total spin density. The dissociation of the C_α−C_β bond in **9** was calculated to be substantially endothermic (95 kJ mol^{-1} relative to **1H**, Table 3) to form the 3-propylguanidine radical (**11**) and glycine enol amide (**10**, Scheme 8). In addition, the C_α−C_β bond cleavage in **9** requires 108 kJ mol^{-1} in the transition state (**TS5**, 130 kJ mol^{-1} relative to **1H**, Table 3), which is notably higher than the TS for the other dissociations of **1H**. An alternative pathway consists of side-chain unfolding in **9** to the linear aminoketyl radical **13** ($\Delta H_{rxn,0} = -2$ kJ mol^{-1}), followed by C_α−C_β bond cleavage in the latter through **TS6** (Scheme S1, Supporting Information). Although **TS6** is 4 kJ mol^{-1} lower in energy than **TS5**, the C_α−C_β bond cleavage remains a high-energy dissociation when compared to the other reaction pathways starting from **1H**.

In contrast to the H migration from the guanidine group that shows it to be a poor H-atom donor, the guanidine radical **1H** is a good receptor for an H atom. A reverse H-atom transfer onto the guanidyl radical necessitates a side-chain folding in **1H** to form conformer **4H** (Scheme 9), which is only slightly less stable than **1H**, e.g. $\Delta G_{g,298}$ (**1H** → **4H**) = 8.9 kJ mol^{-1}. Conformer **4H** then undergoes exothermic transfer of the C_α-hydrogen unto the guanidine sp^2 carbon atom yielding another isomer (**14**, Scheme 9) that is 51 kJ mol^{-1} more stable than **1H** (Table 3). The H-atom transfer in **4H** requires only 47 kJ mol^{-1} (relative to **1H**) in the transition state (**TS7**, Table 3). A further dissociation of **14** proceeds via **TS**8 by β-fission of the C_β−C_γ bond to yield enamine **8** and radical **15** at 83 kJ mol^{-1} threshold energy relative to **1H** (Scheme 9, Table 3).

The TS energies for the competing dissociations of **1H** by loss of H, guanidine-forming N−C_δ bond cleavage, and rearrangements to **9** and **14** were further used to calculate unimolecular rate constants using the RRKM theory. The log *k* plots versus the reactant internal energy are shown in Figure 4. The onsets of the log *k* curves in Figure 4 are close to the respective B3−PMP2/6-311++G(2d,p) TS energies. We note that the onsets from the other high-level calculations are shifted by a few kJ mol^{-1} on the absolute energy scale (Table 3), but their relative positions remain the same. The N−C_δ bond cleavage shows a low-energy onset (Figure 4, curve ***a***). The dissociation becomes observable on the time scale of the experiment (*t*) when the rate constant *k* approaches $1/t = 1.5 \times 10^5$ s^{-1}. For the N−C_δ bond cleavage this occurs at 38 kJ mol^{-1} above the **TS2** energy that determines the kinetic shift for this dissociation.[41] The H atom migration through **TS4** shows a kinetic shift of 60 kJ mol^{-1} (Figure 4, curve ***b***). The most probable internal energy in **1H** can be approximated[42] by the sum of the precursor ion rovibrational enthalpy (34 kJ mol^{-1} at 298 K) and the Franck−Condon energy in vertical electron transfer (68 kJ mol^{-1}) to give $E_{max} \approx 34 + 68 = 102$ kJ mol^{-1}. At this excitation, the RRKM branching ratios favor the N−C_δ bond cleavage (98%) over hydrogen migration (2%) whereas the loss of the guanidinium H is negligible (<10^{-3} %).

The reverse migration through **TS7** of the α-hydrogen atom onto the guanidine sp^2 carbon is the lowest-energy pathway. However, the migration through **TS7** is entropically hampered and shows only a slow increase of log *k* with the reactant internal energy (Figure 4, curve ***d***), such that curves ***a*** and ***d*** cross at 176 kJ mol^{-1} (Figure 4). Note that the N−C_δ bond cleavage can occur in any conformer of **1H** with practically identical transition state energies (cf. **2H** → **TS3**, Table 3) and thus can be viewed as proceeding via multiple, near-degenerate pathways. In contrast, the α-hydrogen atom migration proceeds through a single tight transition state (**TS7**) and this fact further disfavors the migration against the N−C_δ bond cleavage. Intermediate **14**, which is 56 kJ mol^{-1} more stable than **1H** (Table 3), requires 141 kJ mol^{-1} to reach the transition state (**TS8**) for the formation of **8** and **15** (Scheme 9), and this renders this dissociation very slow (Figure 4, curve ***e***). Thus, radical **14** can be viewed as a kinetic trap in dissociations of **1H** in the range of internal energies of 45−176 kJ mol^{-1}. It follows from the kinetic analysis that the N−C_δ bond cleavage remains kinetically

(41) Lifshitz, C. *Mass Spectrom. Rev.* **1982**, *1*, 309−348.
(42) (a) Wolken, J. K.; Tureček, F. *J. Phys. Chem. A* **1999**, *103*, 6268−6281. (b) Wolken, J. K.; Tureček, F. *J. Phys. Chem. A* **2001**, *105*, 8352−8360. (c) Tureček, F. *Int. J. Mass Spectrom.* **2003**, *227*, 327−338.

preferred (>94%) over the other dissociations at **1H** internal energies of up to 400 kJ mol^{-1}.

Discussion

Experiment and theory are in accord that the arginine amide radical **1H** is a bound and observable species. This feature distinguishes arginine radicals from lysine radicals, which are calculated to exoergically dissociate by loss of an ammonium hydrogen atom or rearrange to aminoketyl radicals.[6,43] The stability of **1H** can be attributed to its electronic structure that shows the unpaired electron to be delocalized in a guanidine π-orbital. Upon vertical electron transfer to **1H**$^+$, the incoming electron can reach the *X*-state of the incipient radical that is represented by a Rydberg-like molecular orbital which has a similar nodality as the ground state of ammonium radicals and could promote N−H bond dissociations.[6] Evidently, dissociation from such a transient *X*-state in **1H** is slower than vibrational relaxation that is accompanied by substantial stabilization of the electronic state represented by the guanidine π-orbital. Electron transfer from the Rydberg-like orbital to the π-orbital is likely to be facilitated by the very small energy gap between the *X* and *B* states in the vertically formed **1H** (0.32 eV, 31 kJ mol^{-1}, Figure 3) and the fact that the states must cross early along the internal coordinates involved in the geometry relaxation. An N−H bond dissociation starting from the *X* state represented by the π-orbital requires substantial electron reorganization to reach the transition state in which most of the unpaired electron density (76%) is localized at the departing hydrogen atom.

The other salient feature of **1H** is the substantial transition state energy for the intramolecular hydrogen migration forming the aminoketyl radical **9**. The migrating hydrogen atom carries only about 4% of the unpaired spin density in **1H** which further decreases to 3% in the transition state for the migration (**TS4**). At the same time, 62% of the spin density has been transferred to the amide group in the transition state. This indicates that the hydrogen migration in **1H** can be described as a proton-coupled electron transfer where the electron and proton migrate separately, in the same sense as it was found for lysine and other ammonium radicals.[8,43] Reaching the transition state in **1H** requires mixing the singly occupied molecular orbital (SOMO) of the *X* state with those of excited states to provide a frontier orbital of a requisite nodality (Figure 5). Because of the substantial excitation energy of *X* (e.g., 2.14 eV, 206 kJ mol^{-1} , to the *A* state), this mixing is likely to contribute to the **TS4** energy. In addition, the hydrogen transfer is endoergic. This may also contribute to the relatively high TS energy for the migration in **1H** due to a reorganization of electron density in the doubly occupied bonding orbitals as the molecular geometry changes in the course of the reaction.

The overall result of the electronic properties of the guanidinium radical in **1H** is that the dissociations that are triggered by the H atom migration to the amide group are disfavored against competing N−C$_\delta$ bond cleavage resulting in loss of guanidine and subsequent dissociations of the formed radical intermediate.

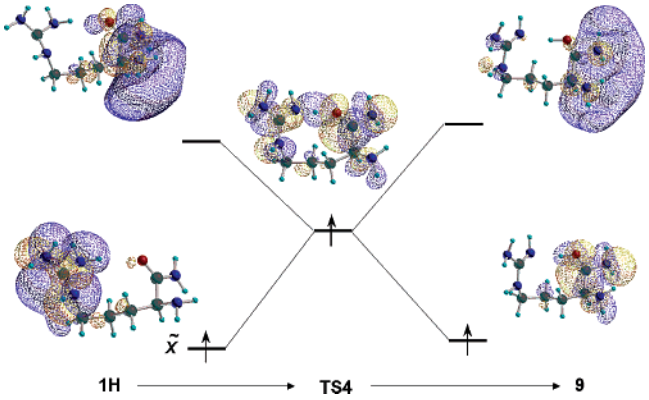

Figure 5. Molecular orbital correlation for N···H···O migration **1H** → **TS4** → **9**.

The results of the current study can be extrapolated to account for the dissociations of arginine-containing peptide ions upon electron capture. A common feature of ECD of arginine-containing peptides is loss of neutral fragments of 59 and 101 Da[44] that are usually assigned to guanidine and (guanidine + C_3H_6).[20,45] These dissociations in peptide cation-radicals are completely analogous to the major dissociation in the neutral radical **1H**, and thus, they do not appear to be critically affected by the presence of additional charges in the peptide cation radicals. The dissociations of peptide N−C$_\alpha$ bonds and formation of ***c*** and ***z***$^\bullet$ fragment ions are known to depend on the peptide composition,[46] sequence,[47] and conformation.[48,49] Anomalous cases have been reported where arginine-containing peptides dissociated by ionic mechanisms on ECD and showed only minor ***c*** and ***z***$^\bullet$ fragment ions.[19] These findings are consistent with the competing nature of the N−C$_\delta$ bond cleavage and H-atom migration that we find for **1H**. Our concurrent study of arginine-containing cation-radicals indicates that the guanidinium group is a poor hydrogen atom donor but a good hydrogen atom acceptor even in the presence of a remote charge at a 10 Å distance.[43] This indicates that N−C$_\alpha$ bond cleavage upon ECD of arginine-containing peptides is not triggered efficiently, and perhaps not at all, by charge-reduction of the protonated guanidine moiety, in contradiction to the Cornell mechanism. The same conclusion can be made for electron-transfer dissociation (ETD) which involves similar species to those treated by ECD. The fact that arginine-containing peptides do undergo N−C$_\alpha$ bond cleavage can be attributed to the UW mechanism involving electron capture in amide π* orbitals that are stabilized by remote charge, which are independent of the electronic nature of the charged group.[6] A point can be made that the facile reverse H atom migration from the C$_\alpha$ position to the guanidyl group that produces C$_\alpha$-radical intermediates may trigger hydrogen exchange[13] and cascade backbone dis-

(43) Radicals derived from ϵ-NH$_2$-protonated lysine amide, N$_\alpha$-acetyl lysine amide, and cation-radicals from doubly protonated N$_\alpha$-glycyl lysine show extremely fast exothermic hydrogen atom migration from the ammonium group to the carbonyl. In contrast, cation-radicals from doubly protonated N$_\alpha$-glycyl arginine show dissociations and rearrangements that are quite analogous to those in **1H**. Tureček, F. Presented at the 54th ASMS Conference on Mass Spectrometry and Allied Topics, Seattle, May 28−June 2, 2006.

(44) Cooper, H. J.; Hudgins, R. R.; Håkansson, K.; Marshall, A. G. *J. Am. Soc. Mass Spectrom.* **2002**, *13*, 241−249.
(45) Cooper, H. J.; Hudgins, R. R.; Håkansson, K.; Marshall, A. G. *Int. J. Mass Spectrom.* **2003**, *228*, 723−728.
(46) Iavarone, A. T.; Paech, K.; Williams, E. R. *Anal. Chem.* **2004**, *78*, 2231−2238.
(47) Mihalca, R.; Kleinnijenhuis, A. J.; McDonnell, L. A.; Heck, A. J. R.; Heeren, R. M. A. *J. Am. Soc. Mass Spectrom.* **2004**, *15*, 1869−1873.
(48) Polfer, N. C.; Haselmann, K. F.; Langridge-Smith, P. R. R.; Barran, P. E. *Mol. Phys.* **2005**, *103*, 1481−1489.
(49) Patriksson, A.; Adams, C.; Kjeldsen, F.; Raber, J.; van der Spoel, D.; Zubarev, R. A. *Int. J. Mass Spectrom.* **2006**, *248*, 124−135.

sociations in arginine-containing peptides, as suggested by O'Connor et al.[14]

In contrast, proton-coupled electron transfer is an extremely facile process in the exothermic H atom migration from a lysine ammonium to the proximate amide group, in line with the Cornell mechanism. The dramatically different behavior of arginine indicates that the Cornell and UW mechanisms are largely complementary, and which one applies is likely to depend on the nature of the charge carriers in the peptide ion. Lysine-containing peptide ions can undergo N−C_α bond cleavage according to both the Cornell and UW mechanisms, although the proportion of dissociations occurring in the ground and excited electronic state may depend on the peptide structure. Arginine-containing peptide ions are predicted to mainly follow the UW mechanism.

Conclusions

Upon femtosecond electron transfer, arginine amide radicals undergo dissociations in the side chain resulting in the loss of guanidine. Products resulting from an intramolecular hydrogen transfer from the protonated guanidine moiety to the amide group are not observed. The experimental results are corroborated by ab initio and density functional calculations that find a large energy barrier for the hydrogen migration from the guanidyl radical to the amide group that makes it kinetically incompetitive with the loss of guanidine. This arginine anomaly allows us to explain the competing ground-state (Cornell) and excited state (Utah−Washington) mechanisms for electron capture and electron transfer dissociations of peptide ions. Both mechanisms are likely to be operational in peptides where the charge carriers are lysine residues, whereas the UW mechanism is predicted to be preferred in peptides where the charge carriers are arginine residues.

Acknowledgment. Support by the National Science Foundation (Grants CHE-0349595 for experiments and CHE-0342956 for calculations) is gratefully acknowledged. Support for the Computational Chemistry Facility at the Department of Chemistry has been jointly provided by the NSF and University of Washington. Thanks are due to Dr. Martin Sadilek and Ms. Eva Fung (Visiting Scholar from the Chinese University of Hong Kong) for technical assistance.

Supporting Information Available: Figure S1 with the reference CID mass spectrum of guanidine cation radical; Tables S1−S22 with optimized geometries in the Cartesian coordinate format; Figures S2−S4 with optimized structures of arginine radicals; Scheme S1. This material is available free of charge via the Internet at http://pubs.acs.org.

JA063676O